

Analysis of boiler-tube erosion by the technique of acoustic emission Part I. Mechanical erosion

L. Zhang^{a,*}, V. Sazonov^a, J. Kent^a, T. Dixon^b, V. Novozhilov^a

^a Department of Mechanical and Mechatronic Engineering, The University of Sydney, Sydney NSW 2006, Australia

^b Sugar Research Institute, Mackay, Qld, Australia

Abstract

This paper investigates the mechanical erosion of the metal tubes in bagasse-fired boilers with the aid of the acoustic emission technique. By studying the material removal under various collision conditions, the paper analyzes the dependence of the erosion wear upon the impact angle, velocity, size and concentration of the particles. It was found that the material removal mechanisms were mainly dependent on the particle collision angle and fell into four regimes characterized by rubbing and scratching, cutting and cracking, forging and extrusion as well as sputtering and adhesion. The highest wear rate took place with the cutting and cracking mechanism when the particle collision angle was in the range of 20–30°. The variation of the acoustic emission energy confirmed the conclusions. Finally, three simple formulae were developed to show the dependence of the erosion wear upon the main erosion parameters. © 2001 Elsevier Science B.V. All rights reserved.

Keywords: Mechanical erosion; Acoustic emission; Boiler-tube

1. Introduction

Erosion of metal tubes in bagasse-fired boilers is a problem in the sugar industry, causing considerable maintenance cost, because the combusted bagasse-particles, with the characteristic dimensions from a few microns to millimeters, erode the tubes with high speeds, ranging from 10 to 30 m/s, and result in significant wear. However, a boiler structure is so complicated that the situation of the particle-tube interaction associated with the turbulent two-phase flow becomes hard to model. In different parts of a boiler, the tubes can experience diverse erosion conditions, such as different particle angularity, impact angle, impact speed, particle concentration, particle size distribution and temperature change. All these make an erosion prediction very difficult.

Erosion of metal parts is a common problem in industry, such as in coal-fired turbines, fluidized beds and boiler-tubes. Over the last 40 years, many models have been proposed to evaluate the rate of material removal under various eroding conditions (e.g. [1–9]). However, each of these models focused only on one or two mechanisms of the material removal and thus none is adequate alone in terms of wear prediction for the specific boiler-tube erosion at elevated temperatures. In a boiler, because the ash-tube interactions occur under very different conditions, a model that fails to

take into account the locations of the interaction, densities of impacts, energy of impingement and so on cannot be practical. This raises further difficulties for a reliable and feasible evaluation of the boiler-tube erosion. To understand the erosion mechanism of the metal tubes in bagasse-fired boilers, therefore, a sophisticated method must be developed to explore both the individual and coupled effects of the key variables that govern the erosion process. In addition, the erosion on a boiler piping system occurs at different locations, which are hard to be detected when the boiler is operating.

The acoustic emission technique seems to be a useful tool to resolve the above problems. A major advantage of an acoustic emission inspection is that it allows the whole structure to be monitored at the same time with simple in situ set-ups. The analysis does not need the scanning of individual defects, but uses a set of acoustic sensors that are attached to the structure, directly or indirectly, to transmit acoustic signals. A wide range of dynamic parameters can then be observed throughout an erosion process. Relevant investigations have reported that the emission of dislocations, initiation of cracks and dynamic response to an impact can be successfully detected by this method (e.g. [9–13]). However, no model is available so far to link the material removal with the acoustic signals for predicting the erosion wear, although some studies have shown that a relationship does exist between the signals and the particle impingement (e.g. [14,15]).

* Corresponding author. Tel.: +61-2-9351-2835; fax: +61-2-9351-7060.
E-mail address: zhang@mech.eng.usyd.edu.au (L. Zhang).

Nomenclature

a, b	multivariable regression coefficients (Eqs. (2) and (4))
c	particle concentration, defined as the mass of the particles per unit volume in the air-stream
d	average diameter of a particle
E_n	acoustic emission energy measured
H	hardness of the tube material
V	impact velocity of a particle

Greek letters

α	particle collision angle, defined in Fig. 1
ρ	density of the particle material
τ	erosion time
ξ	erosion wear, defined as the mass loss of the tube material after mechanical erosion

The purpose of this work is to understand the material removal mechanisms and establish a relationship between the erosion variables and those of acoustic emission. Based on this relationship, the mechanical erosion at room temperature will be characterized. Investigations into the problem at elevated temperatures will be discussed in the next part of the series research.

2. Experimental details

The apparatus particularly constructed for the mechanical erosion experiment in this study is shown in Fig. 1, consisting of (1) the air compressor, (2) the pressure regulator, (3) the flow meter, (4) the nozzle (16 mm in diameter), (5) the particle container, (6) the tube specimen (63 mm in diameter), (7) the particle collector, (8) the acoustic sensor, (9) the amplifier and (10) the computer. The erodent particles, which were collected from the actual boiler under study, were fed from the particle container (5) to a feeding plate that had six channels through which the particles were fed into the nozzle by the pressurized air-stream. The channels were with different dimensions so that the particle concentration could be adjusted in the experiment. The air pressure was also adjustable via the pressure regulator (2), which altered the stream velocity from 0 to 30 m/s. The stream was directed through the nozzle onto the surface of the specimen (6) that was exactly the boiler-tube material (AISI1015 steel). The axis of the nozzle is always aligned with the diameter axis of

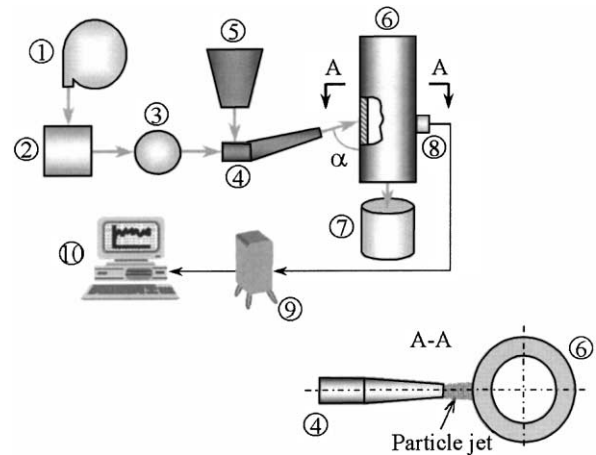


Fig. 1. Experimental set-up.

the tube, as illustrated by section A–A in Fig. 1, but the angle of the nozzle with respect to the longitudinal axis of the tube was variable from 0 to 90° so that the collision angle of the particle jet, α , was controlled. The acoustic sensor (8), of the type S9215 that is reliable below 540°C, was directly attached to the pipe wall opposite to the nozzle to minimize the loss of the acoustic energy in measurement. The impact signals detected by the sensors were then sent, as a voltage output, to the computer (10) through the amplifier (9) for analysis, using the MISTRAS (Massively Instrumented Sensor Technology with Received Acoustic Signal) software [16]. The energy thus measured by the acoustic system is a fraction of the impact energy dissipated in the tube material during the process of particle–tube interaction.

After an erosion test, the amount of the material removed was measured by a microbalance with a resolution of 10 μg . The erosion wear rate was calculated based on at least five repeated experiments in which the particle collision velocity, collision angle and concentration remained identical nominally. The average deviation of the repeated measurements was 5%. The mechanical properties of the particle and tube materials are listed in Table 1.

3. Results and analysis

The geometry of the ash particles is angular with sharp corners, as shown in Fig. 2, and hence, they may scratch or cut a specimen surface during particle–tube interactions. The particles were the pulverized bagasse after combustion and were composed of a mixture of inorganic elements, mostly

Table 1
Mechanical properties of the particle and tube materials [17]

	Hardness (GPa)	Elastic modulus (GPa)	Poisson's ratio	Density (kg/m^3)
Particle	4.0	–	0.17	1.6×10^3
Tube steel (AISI1015)	2.0	210	0.29	7×10^3

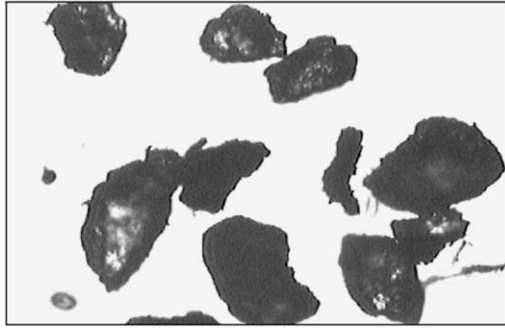


Fig. 2. Geometry of ash particles.

silicon oxide, according to an X-ray diffraction analysis, and some organic elements that were soft and could not wear the tube material directly mechanically. A fraction separation showed that the ash particles in the boiler were mainly of the dimensions between 80 and 250 μm in diameter. The size distribution of the particles is summarized in Table 2.

To understand the effect of curvature of the tube specimens on erosion, a series of tests on flat plates made of the tube material were also carried out. The results showed that under the same erosion conditions, the difference in the amount of wear was always within 0.5%, which is negligible. This is because the particle jet size is much smaller than the tube diameter and inside the jet impact area the tube surface can be regarded as nearly flat. Thus for convenience, the circumferential curvature of a tube surface will be ignored in the following discussion.

3.1. Effect of collision angle

The collision angle of the particles plays an important role in the tube erosion process. Fig. 3 shows its effect on the amount of wear with various particle concentrations when the particle velocity, particle size and erosion time remained unchanged. The complicated variation of the curves indicates that the mechanism of the material removal must have changed when the particle collision angle varies. The wear is small when the angle is small, reaches its maximum when it varies between 20 and 30° and decreases steadily until the angle becomes 80°. When α increases further, the wear increases again. The scanning electron micropho-

Table 2
Size distribution of the boiler ash-particles

Average diameter of particles (μm)	Percentage per unit volume
50–80	11.8
80–100	12.2
100–212	44.5
212–250	23.4
250–355	4.7
355–425	2.8
425–500	0.6

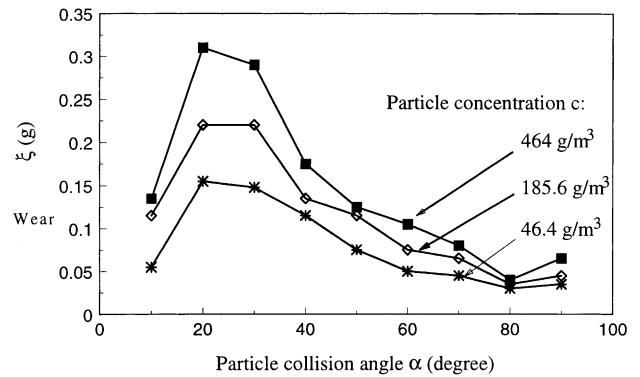


Fig. 3. Variation of material removal with particle collision angle. The erosion conditions are $V = 20\text{ m/s}$ and $\tau = 52\text{ min}$ with the mixed particles (Table 2).

tographs of the tube surfaces after erosion, Fig. 4, show valuable evidence for recognizing the mechanism change of the material removal.

At a low collision angle, 10° say, the material removal was mainly by rubbing and scratching, as shown by the ductile rubbing and scratching traces on the surface (Fig. 4a). The phenomenon of plastic extrusion tangential to the eroded surface, which generates microscales, is also obvious. In this case, the impact force normal to the tube surface is very small, the plastic deformation thus caused in the tube subsurface is shallow and hence the wear is light although the tangential component of the impact force is large.

At a collision angle between 20 and 30°, cutting becomes one of the major mechanisms of the material removal. On the eroded surfaces with α equal to 20 and 30°, respectively, deformation via chipping is a characteristic, as shown in Fig. 4b and c. This is because in this range of collision angles the component of the impact force normal to the tube surface becomes great enough to enable a particle to penetrate into the tube material while the component tangential to the surface is still sufficient to proceed the cutting. In addition, cracking has also appeared to assist the material removal, as shown in Fig. 4c, which is related to the tensile surface stress behind a cutting particle, generated by the cutting. Obviously, the cutting together with the cracking serves as the most effective material removal mode in the mechanical erosion. That is why ξ reaches its maximum when α varies in the range of 20–30°.

The cutting mode of the material removal becomes minor when α increases further. The residual deformation shown in Fig. 4d, which is the result of $\alpha = 60^\circ$, shows that extrusion out of the tube surface is the major mechanisms. Such extrusion was due to the particles microforging operations under the relatively large particle impingement angle. When this deformation mode becomes dominant, it is reasonable to see from Fig. 3 that the amount of material removal becomes smaller and smaller.

When the collision angle is beyond 80°, the tangential component of a particle impact decreases quickly. As a

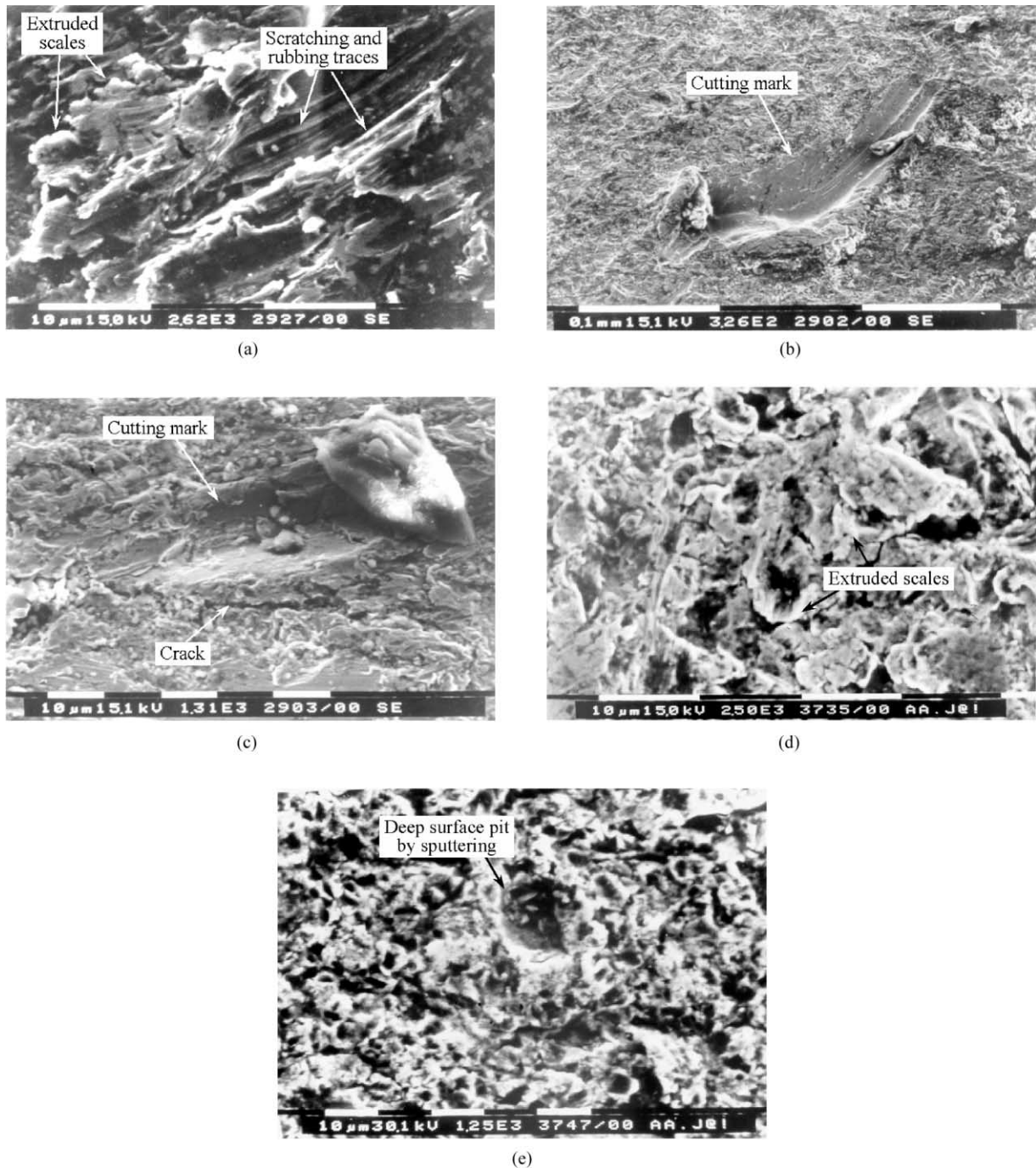


Fig. 4. SEM micrographs of the eroded surfaces subjected to different collision angles (α): (a) 10° , (b) 20° , (c) 30° , (d) 60° , (e) 90° . The erosion conditions were $V = 20$ m/s, $\tau = 5$ min and $d = 250$ μ m.

result, neither the cutting nor the scratching and rubbing are likely to happen. The main deformation is via forging and the almost normal extrusion associated with the forging, as shown in Fig. 4e. The larger surface dips may be generated by sputtering, when a local crack forms due to residual stresses after the particle impacts and thus the material sputters, or adhesion, when the tube material adheres to a flying particle at its impact and is carried away by the particle. To clarify this phenomenon, an impact normal to

the tube surface with a single particle is particularly carried out experimentally. The result, Fig. 5, confirms that the sputtering-adhesion is indeed the mechanism of the surface pit formation. Because of the occurrence of the sputtering and adhesion, ξ gets greater as α becomes larger than 80° .

The above observations are related to the acoustic emission energy recorded, which, as stated previously, is a fraction of the energy loss during the particle–tube interaction. It is obvious from Fig. 6 that the deformation caused by

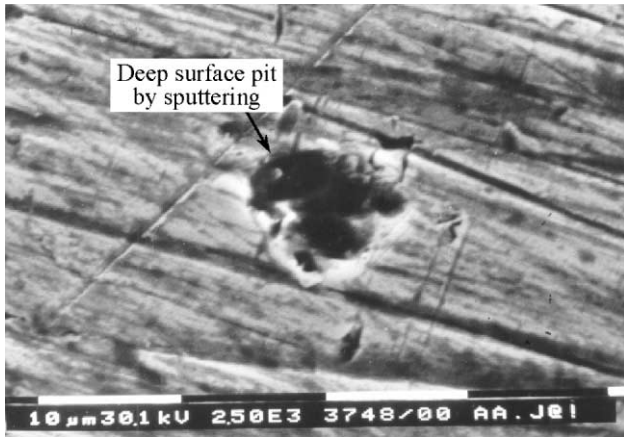


Fig. 5. A surface dip formed by sputtering or adhesion when the tube was under a vertical impact ($\alpha = 90^\circ$) by a single particle of $d = 425 \mu\text{m}$ at $V = 30 \text{ m/s}$.

rubbing and scratching at a lower collision angle α dissipates greater energy than that via cutting and cracking when α ranges from 20 to 30° . When the forging and extrusion mode becomes dominant, the energy dissipation rises. These are consistent with the general theory of machining.

3.2. Effect of particle size

Under a given impact velocity, concentration and collision angle, the particle size has a significant effect on the amount of wear, ξ , as shown in Fig. 7. With the erosion conditions specified, particles with diameters below $50 \mu\text{m}$ do not cause measurable wear. The larger the particle size, the greater the erosion wear is (Fig. 7a). Moreover, ξ is roughly a linear function of erosion time τ , (Fig. 7b) regardless of the particle dimension. As just discussed, the material removal by mechanical erosion is directly through the mechanism of cutting, adhesion, forging–extrusion, etc. or due to their combinations. Here, the stable and linear variation of the material removal with respect to τ indicates that the mechanical properties of the surface layer material of the

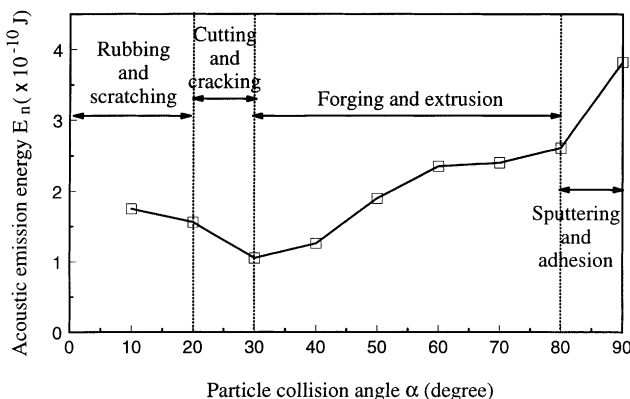


Fig. 6. Variation of erosion energy with collision angle.

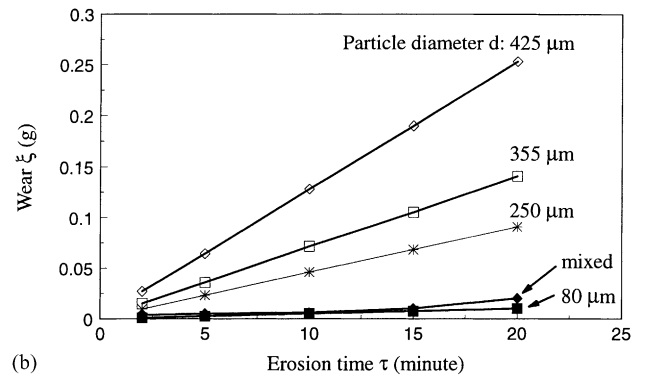
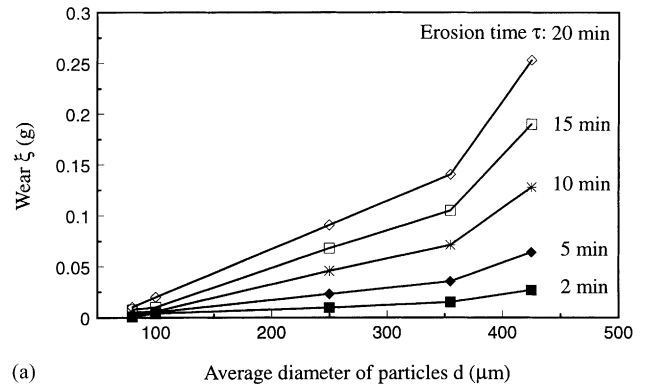


Fig. 7. Effect of particle size on erosion wear at various erosion time. The erosion conditions are $V = 20 \text{ m/s}$, $c = 185.6 \text{ g/m}^3$ and $\alpha = 90^\circ$.

tube specimen have been stabilized very quickly under the particle impingement. The mechanism of the material removal then remains unchanged with the increment of erosion time. This seems to be true for all the particle sizes studied. It is also interesting to note that when the average particle diameter is $< 350 \mu\text{m}$, the amount of wear increases approximately linearly with the particle size, as shown in Fig. 7a. However, beyond $350 \mu\text{m}$, the effect of particle size becomes stronger, leading to an increase of material removal and suggesting that a change of the material removal mechanism may have occurred due to the change of the particle impact energy.

3.3. Effect of particle concentration

In this study, the particle concentration c is defined as the mass of the particles per unit volume in the pressurized air-stream. Thus at a given velocity, high c means more particle impacts onto the tube surface in a given time span. As shown in Fig. 8, the increase of particle concentration promotes erosion wear in general. This is straightforward because erosion with more particles within a given period of time will certainly remove more materials. However, the effect of particle concentration is very related to the dominant mechanism of wear when the particle collision angle

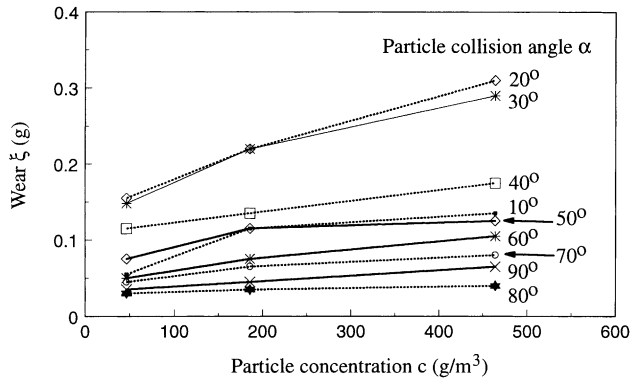


Fig. 8. Effect of particle concentration on erosion wear with erosion conditions of $V = 20$ m/s, $\tau = 52$ min and mixed particle distribution listed in Table 2.

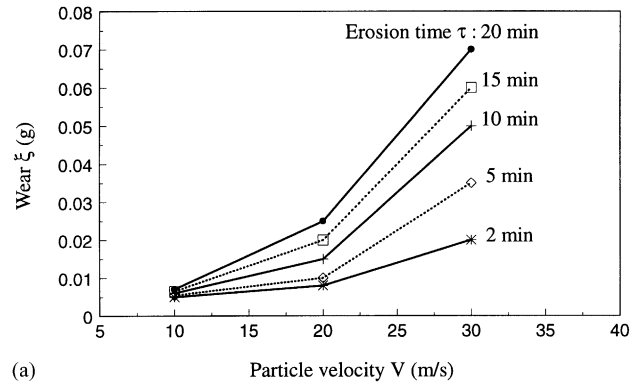
changes. If rubbing, scratching, forging or extrusion governs the material removal, the dependence of erosion wear upon the increase of c is rather moderate, see for instance the curves with $\alpha = 10^\circ$ and 50° – 90° . But in the regime where cutting and cracking dominate, the increment of particle concentration promotes the tube wear, see the curves with $\alpha = 20$ and 30° . It is worthwhile to note that when sputtering or adhesion appears between $\alpha = 80$ and 90° , the effect of concentration becomes stronger.

3.4. Effect of particle velocity

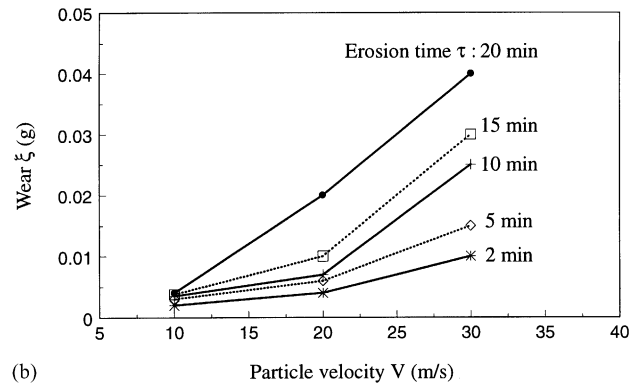
The effect of particle velocity, V , on the material loss was studied with a fixed value of particle concentration of 185.6 g/m^3 . Fig. 9 shows that the amount of wear is a monotonic increasing function of V at various erosion time τ under all the particle collision angles. This is reasonable because a particle with a higher speed carries greater energy and in turn deforms the tube material more upon impingement. Once again, however, the extent of the velocity effect depends on the material removal mechanism involved, which is similar to the effect of particle concentration. For example, the slopes of the curves in Fig. 9a, where the wear is caused by the cutting-cracking mechanism because $\alpha = 20^\circ$, are generally greater than those in Fig. 9b with the sputtering-adhesion mechanism because $\alpha = 90^\circ$.

3.5. Evaluation of erosion wear

The above discussion has shown the mechanisms of the boiler-tube deformation under mechanical erosion and the qualitative dependence of wear upon various erosion conditions. Due to the complexity of the erosion process, it is difficult to get a theoretical solution to quantitatively describe the variation of erosion wear. However, recent success in the modeling of precision polishing of plastic lenses [18] using dimensional analysis, which also involves material removal by irregularly shaped abrasives, suggests that it is possible



(a)



(b)

Fig. 9. Effect of particle velocity on erosion wear. The erosion conditions are $c = 185.6 \text{ g/m}^3$ with mixed particle distribution listed in Table 2. The collision angles (α): (a) 20° , (b) 90° .

to obtain an empirical relationship for an approximate evaluation of the boiler-tube erosion.

3.5.1. Relationship of wear with erosion variables

The variables which affect the amount of erosion wear, ξ , as understood from the previous discussion, are the particle velocity V , particle diameter d , collision angle α , particle concentration c , erosion time τ and the property parameters of both the particle and tube materials, such as the hardness and density. However, because the relative properties of the tube and particle materials remain constant during the mechanical erosion in the present erosion system, the ratios of the corresponding material parameters, such as the ratio of the tube hardness to that of the particle, do not need to be regarded as the variables in the dimensional analysis. In addition, the environmental humidity and temperature in the present erosion system are also constant, and thus, their effects can be ignored. The dimensional formulae of the above variables are listed in Table 3, where only the particle density ρ and tube hardness H are taken as the material variables because the former is related to the impact energy of a particle and the latter represents the plastic deformation property of the tube material.

The π -theorem of dimensional analysis can be used to form all the independent nondimensional products. In the

Table 3
Dimensional formulae of the erosion variables

Erosion variable	Symbol	Dimensional formula
Erosion wear (mass loss)	ξ	[M]
Erosion time	τ	[T]
Particle velocity	V	[LT ⁻¹]
Particle concentration (mass of particles per unit volume in air-stream)	c	[ML ⁻³]
Particle collision angle	α	0
Average diameter of a particle	d	[L]
Hardness of the tube material	H	[ML ⁻¹ T ⁻²]
Density of the particle material	ρ	[ML ⁻³]

present case, as shown in Table 3, there are eight erosion variables and three primary units that are mass [M], length [L] and time [T]. However, the collision angle α is already dimensionless. This means that there exist only four independent nondimensional products that need to be constructed from the seven remaining variables. A standard dimensional analysis using the dimensional formulae in Table 3 leads to

$$\frac{\xi}{\rho d^3} = f\left(\frac{c}{\rho}, \frac{d}{\tau\sqrt{H/\rho}}, \frac{V}{\sqrt{H/\rho}}, \alpha\right), \quad (1)$$

where f is an undetermined function. However, it is seen from Fig. 3 that the relationship between ξ and α can be described by a polynomial. Thus Eq. (1) may be approximately expressed as

$$\frac{\xi}{\rho d^3} \sim \left(\frac{c}{\rho}\right)^k \left(\frac{d}{\sqrt{H/\rho}\tau}\right)^l \left(\frac{V}{\sqrt{H/\rho}}\right)^m \left(\sum_{i=0}^n a_i \alpha^i\right) \quad (2)$$

where k, l, m, n and a_i ($i = 1, \dots, n$) are constants that can be determined by the multivariable regression method. A numerical calculation using the experimentally measured data gives rise to $k = 0.2, l = -1, m = 2, n = 6, a_0 = -2.189 \times 10^{-9}, a_1 = 2.221 \times 10^{-8}, a_2 = -4.169 \times 10^{-8}, a_3 = 2.145 \times 10^{-8}, a_4 = 1.213 \times 10^{-8}, a_5 = -1.540 \times 10^{-8}$ and $a_6 = 4.045 \times 10^{-9}$. The experimental data gather around a straight line, as shown in Fig. 10, where the horizontal axis is

$$\mathcal{E} = \left(\frac{c}{\rho}\right)^{0.2} \left(\frac{d}{\sqrt{H/\rho}\tau}\right)^{-1} \left(\frac{V}{\sqrt{H/\rho}}\right)^2 \left(\sum_{i=0}^6 a_i \alpha^i\right).$$

Eq. (2) shows approximately the functional dependence of the boiler-tube wear under mechanical erosion upon the major erosion variables.

3.5.2. Relationship of wear with acoustic emission energy

From the point of view of monitoring the tube erosion of a running boiler by the acoustic emission, it is important to establish a direct relationship between the amount of wear, ξ , and the acoustic emission energy measured, E_n . Fig. 6 has shown that E_n is indeed related to the erosion mechanisms

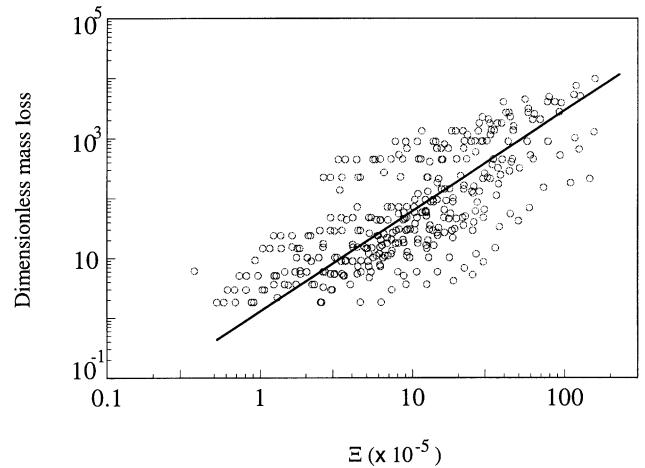


Fig. 10. Master curve of erosion wear.

and thus by dimensional analysis a functional relationship similar to Eq. (2) may also be possible. With the same considerations in obtaining Eq. (2), all the variables in Table 3 can still be used provided that ξ in the table is replaced by E_n that has the dimensional formula of [ML²T⁻²]. As a result, it leads to

$$\frac{E_n}{Hd^3} = g\left(\frac{c}{\rho}, \frac{d}{\tau\sqrt{H/\rho}}, \frac{V}{\sqrt{H/\rho}}, \alpha\right), \quad (3)$$

where g is an undetermined function. Similar to Eq. (2), an approximate expression of Eq. (3) may also be taken as

$$\frac{E_n}{Hd^3} \sim \left(\frac{c}{\rho}\right)^{k'} \left(\frac{d}{\tau\sqrt{H/\rho}}\right)^{l'} \left(\frac{V}{\sqrt{H/\rho}}\right)^{m'} \left(\sum_{i=0}^{n'} b_i \alpha^i\right), \quad (4)$$

where k', l', m', n' and b_i ($i = 1, \dots, n'$) are constants to be determined. Again, a numerical regression using the

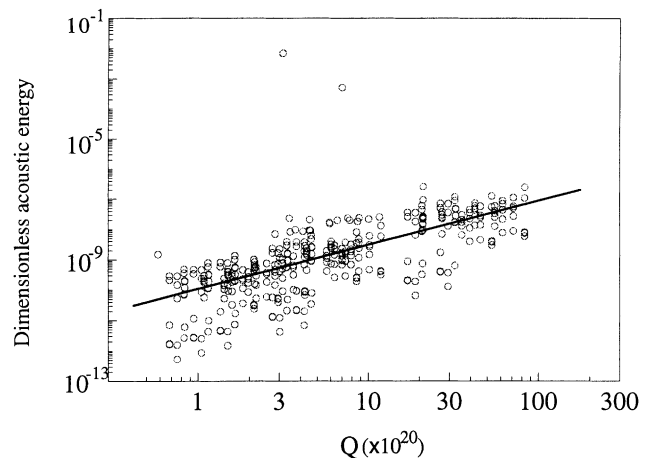


Fig. 11. Master curve of erosion energy.

measured data gives rise to $k' = 0.2$, $l' = -2$, $m' = 2$, $n' = 6$, $b_0 = 1.136 \times 10^{-11}$, $b_1 = 2.969 \times 10^{-10}$, $b_2 = -1.695 \times 10^{-9}$, $b_3 = 3.908 \times 10^{-9}$, $b_4 = -4.105 \times 10^{-9}$, $b_5 = 2.012 \times 10^{-9}$ and $b_6 = -3.736 \times 10^{-10}$. Fig. 11 shows that the experimental measurements also collapse roughly to a straight line, where

$$\Theta = \left(\frac{c}{\rho}\right)^{0.2} \left(\frac{d}{\tau\sqrt{H/\rho}}\right)^{-2} \left(\frac{V}{\sqrt{H/\rho}}\right)^2 \left(\sum_{i=0}^6 b_i \alpha^i\right).$$

Formula (4) correlates the acoustic emission energy, which is directly measurable, to the erosion parameters.

The relationship of wear in terms of the acoustic energy is given by the ratio of Eq. (1)–(3), if functions f and g are determined exactly, i.e.

$$\xi = \frac{\rho}{H} \frac{f}{g} E_n \quad (5)$$

4. Conclusions

With the aid of the acoustic emission technique, this paper investigated the material removal mechanisms in the mechanical erosion of the boiler-tubes caused by the bagasse-ash particles. The study led to the following major conclusions:

1. There exist four regimes with different governing mechanisms of material removal. They are rubbing and scratching regime when the particle collision angle α is below 20° , cutting and cracking regime when α is between 20° and 30° , forging and extrusion regime when α varies from 30° to 80° and sputtering and adhesion regime when the angle is beyond 80° , but $<90^\circ$. However, since the transition from one regime to the other is gradual, the above boundary division is not absolutely exact.
2. The simple formulae developed by the dimensional analysis, i.e. Eqs. (2), (4) and (5), show approximately the dependence of the erosion wear upon the main erosion parameters.

It is worthwhile to recall that the coefficients in formulae (2) and (4) were determined by the data from the specific erosion system with bagasse-particles and AISI1015 steel tubes. Their values should be examined when the formulae are to apply to other erosion systems with different particle and target materials, although the formulae are nondimensional.

Acknowledgements

This work was financially supported by the Australia Research Council and the Sugar Research Institute through a SPIRT Grant.

References

- [1] E. Raask, *Erosion Wear in Coal Utilization*, Hemisphere, Washington, 1988, p. 8–9.
- [2] M. Talia, H. Lankarani, J.E. Talia, New experimental technique for the study and analysis of solid particle erosion mechanisms, *Wear* 225–229 (1999) 1070–1077.
- [3] A. Levy, The erosion-corrosion of tubing steels in combustion boiler environments, *Corrosion Sci.* 35 (1993) 1035–1056.
- [4] W.P. Bauver, T.C. McGough, A facility of the characterization of erosion of heat transfer tubing, *Gas–Solid Flow*, ASME, New York, 1984, pp. 115–122.
- [5] B.A. Lindsley, A.R. Marder, The effect of velocity on the solid particle erosion rate of alloys, *Wear* 225–229 (1999) 510–516.
- [6] Y. Xie, H.McI. Clark, H.M. Hawthorne, Modelling slurry particle dynamics in the Coriolis erosion tester, *Wear* 225–229 (1999) 405–416.
- [7] I. Finnie, The mechanism of erosion of ductile metals, in: *Proceedings of the Third National Congress of Applied Fluid Mechanics*, Trans., ASME, STR664 (1958) 527–532.
- [8] W.J. Head, M.E. Harr, The development of a model to predict the erosion of materials by natural contaminants, *Wear* 15 (1970) 1–46.
- [9] R. Bellman, A. Levy, Erosion mechanism in ductile metals, *Wear* 70 (1981) 1–27.
- [10] R.K. Miller, P. McIntire (Eds.), *Nondestructive Testing Handbook, Acoustic Emission Testing*, Second Edition, Vol. 5, American Society for Nondestructive Testing, OH, 1987, pp. 275–310.
- [11] A.A. Polock, Acoustic emission amplitude distributions, *Int. J. Advances Nondestructive Testing* 7 (1981) 215–239.
- [12] D.J. Buttle, C.B. Scruby, Characterization of particle impact by quantitative acoustic emission, *Wear* 137 (1990) 63–93.
- [13] D. Koch, Multichannel spectral analysis for tube leak detection, *IEEE* 39 (1993) 522–532.
- [14] Y.I. Oka, M. Matsumura, T. Kawabata, Relationship between surface hardness and erosion damage caused by solid particle impact, *Wear* 162–164 (1993) 688–695.
- [15] D.L. Parry, Industrial application of acoustic emission analysis technology, in: J.C. Spanner, J.W. McElroy (Eds.), *Monitoring Structural Integrity by Acoustic Emission*, STR571, American Society for Testing and Materials, Baltimore, 1975, pp. 150–183.
- [16] Physical Acoustics Corporation, *MISTRAS 2001 AEDSP-32/16 User's Manual*, Princeton, NJ, 1995.
- [17] British Standards for Steel and Steel Products, *BS Handbook No.10*, British Standards Institution, London, 1949, pp. 350–351 and 516–521.
- [18] J. Sun, L.C. Zhang, Y.-W. Mai, S. Payor, M. Hogg, material removal evaluation in the optical polishing of hydrophilic polymer materials, in: L.C. Zhang, N. Yasunaga (Eds.), *Advances in Abrasive Technology*, World Scientific, Singapore, 1997, pp. 76–80.